

Title	FIRST SIMULTANEOUS OBSERVATION OF AN H MORETON WAVE, EUV WAVE, AND FILAMENT/PROMINENCE OSCILLATIONS
Author(s)	Asai, Ayumi; Ishii, Takako T.; Isobe, Hiroaki; Kitai, Reizaburo; Ichimoto, Kiyoshi; UeNo, Satoru; Nagata, Shin'ichi; Morita, Satoshi; Nishida, Keisuke; Shiota, Daikou; Oi, Akihito; Akioka, Maki; Shibata, Kazunari
Citation	The Astrophysical Journal (2012), 745(2)
Issue Date	2012-02-01
URL	<a href="http://hdl.handle.net/2433/153980">http://hdl.handle.net/2433/153980</a>
Right	© IOP Publishing 2012
Type	Journal Article
Textversion	author

## First Simultaneous Observation of H $\alpha$ Moreton Wave, EUV Wave, and Filament/Prominence Oscillations

Ayumi Asai<sup>1</sup>, Takako T. Ishii<sup>2</sup>, Hiroaki Isobe<sup>1</sup>, Reizaburo Kitai<sup>2</sup>, Kiyoshi Ichimoto<sup>2</sup>, Satoru UeNo<sup>2</sup>, Shin'ichi Nagata<sup>2</sup>, Satoshi Morita<sup>2</sup>, Keisuke Nishida<sup>2</sup>, Daikou Shiota<sup>3</sup>, Akihito Oi<sup>4</sup>, Maki Akioka<sup>5</sup>, and Kazunari Shibata<sup>2</sup>

asai@kwasan.kyoto-u.ac.jp

### ABSTRACT

We report on the first simultaneous observation of an H $\alpha$  Moreton wave, the corresponding EUV fast coronal waves, and a slow and bright EUV wave (typical EIT wave). Associated with an X6.9 flare that occurred on 2011 August 9 at the active region NOAA 11263, we observed a Moreton wave in the H $\alpha$  images taken by the Solar Magnetic Activity Research Telescope (SMART) at Hida Observatory of Kyoto University. In the EUV images obtained by the Atmospheric Imaging Assembly (AIA) on board the *Solar Dynamic Observatory* (SDO) we found not only the corresponding EUV fast “bright” coronal wave, but also the EUV fast “faint” wave that is not associated with the H $\alpha$  Moreton wave. We also found a slow EUV wave, which corresponds to a typical EIT wave. Furthermore, we observed, for the first time, the oscillations of a prominence and a filament, simultaneously, both in the H $\alpha$  and EUV images. To trigger the oscillations by the flare-associated coronal disturbance, we expect a coronal wave as fast as the fast-mode MHD wave with the velocity of about 570 – 800 km s<sup>-1</sup>. These velocities are consistent with those of the observed Moreton wave and the EUV fast coronal wave.

---

<sup>1</sup> Unit of Synergetic Studies for Space, Kyoto University, Yamashina, Kyoto 607-8471, Japan.

<sup>2</sup> Kwasan and Hida Observatories, Kyoto University, Yamashina, Kyoto 607-8471, Japan.

<sup>3</sup> Advanced Science Institute, RIKEN, Wako, Saitama 351-0198, Japan.

<sup>4</sup> College of Science, Ibaraki University, Mito, Ibaraki 310-8512, Japan.

<sup>5</sup> Hiraiso Solar Observatory, National Institute of Information and Communications Technology, Hitachinaka, Ibaraki 311-1202, Japan.

*Subject headings:* Magnetohydrodynamics (MHD) — Shock waves — Sun: corona  
 — Sun: filaments, prominences — Sun: flares

## 1. Introduction

Moreton waves, flare-associated waves seen in  $H\alpha$ , have been observed (Moreton 1960; Smith & Harvey 1971; Shibata et al. 2011) to propagate in restricted angles with the velocity of about  $500 - 1500 \text{ km s}^{-1}$ . They sometimes show arc-shaped fronts, and are often associated with type-II radio bursts (Kai 1970). They are transient, and appear only for about 10 minutes. Associated with flares, remote filaments and prominence are sometimes activated or excited to oscillate. These “winking filaments” are also thought to be caused by flare-associated waves, and are called as invisible Moreton waves (Smith & Harvey 1971; Tripathi et al. 2009; Hershaw et al. 2011). After the findings, Uchida (1968) suggested that Moreton waves are the intersection of the fast-mode magnetohydrodynamic (MHD) shock propagating in the corona with chromosphere. This model has been widely accepted, and the coronal counterparts have been surveyed for a few decades. Moreton waves are rare to be observed even for large flares (Shibata et al. 2011).

After the launch of the *Solar and Heliospheric Observatory (SOHO)*, the EUV Imaging Telescope (EIT) found wavelike phenomena associated with flares, which are called “EIT waves” (Thompson et al. 1999, 2000). Although EIT waves were expected to be the coronal counterpart of Moreton waves, they show different physical characteristics from those of Moreton waves: the propagating velocity is much slower than that of Moreton wave and is about  $200 - 400 \text{ km s}^{-1}$ , the lifetime is much longer and is about 45 – 60 minutes, they can show isotropic propagation, while Moreton waves propagate with restricted angles (Klassen et al. 2000; Warmuth 2007; Thompson & Myers 2009). There have been, therefore, remained a question whether EIT waves are really coronal counterparts of Moreton waves or no. As for searching for a coronal counterpart of Moreton waves, the Soft X-ray Telescope (SXT) on board *Yohkoh* found wavelike phenomena in soft X-rays, called X-ray waves (Khan & Hudson 2000; Khan & Aurass 2002). X-ray waves are confirmed to be a real counterpart of Moreton waves by simultaneous observations of X-ray waves and Moreton waves (Narukage et al. 2002, 2004).

Then, we come to an issue what EIT waves are. Eto et al. (2002) clearly showed that an EIT wave is different from a Moreton wave, based on simultaneous observations of them. On the other hand, Warmuth et al. (2004a,b) argue that the velocity discrepancy of EIT and Moreton waves can be explained by the deceleration of coronal waves. The mechanism of EIT waves remains, therefore, very controversial (Warmuth 2007; Wills-Davey & Attrill

2009; Gallagher & Long 2010). Delannée & Aulanier (1999) and Chen et al. (2002, 2005) proposed the field-line stretching model for EIT waves. They suggested that EIT bright fronts were not “waves” at all, but instead plasma compression at stable flux boundaries due to rapid magnetic field expansion. This model can also resolve the puzzle why EIT waves often stop at magnetic separatrices.

Recently, by the Atmospheric Imaging Assembly (AIA; Title & AIA team 2006, Lemen et al. 2011) on board the *Solar Dynamic Observatory* (*SDO*), fast coronal waves have been observed associated with flares (e.g. Liu et al. 2010; Ma et al. 2011). These waves (hereafter called “EUV fast coronal waves”) are thought to be the fast-mode MHD waves. Coronal X-ray waves and EUV fast coronal waves have been also observed spectroscopically with the EUV Imaging Spectrometer (EIS) on board *Hinode* (Asai et al. 2008; Harra et al. 2011).

Chen & Wu (2011) found two different coexisting coronal waves, slow coronal wave (i.e. EIT wave) and fast coronal wave, from EUV observations taken by *SDO/AIA*. Although the fast coronal wave seems to be the coronal counterpart of a Moreton wave, they used only EUV images, and it remained to be confirmed whether it is a classical  $H\alpha$  Moreton wave. This letter presents the first simultaneous observation of EUV waves and a Moreton wave by using EUV and  $H\alpha$  images with high spatial and temporal resolutions. Moreover, we found not only a winking filament on the disk, but also an oscillating prominence on the limb, triggered by the coronal wave (Moreton wave).

## 2. Observations

An intense flare, X6.9 on the *GOES* scale, occurred on 2011 August 9 at the Active Region NOAA 11263 (N17°, W71°). The flare started at 07:48 UT, and peaked at 08:05 UT. Associated with the flare, we observed a Moreton wave in the  $H\alpha$  images obtained by the Solar Magnetic Activity Research Telescope (SMART; UeNo et al. 2004), at Hida Observatory, Kyoto University, Japan. SMART regularly observes the full-disk sun in seven wavelengths around the  $H\alpha$  line (6562.8 Å), i.e.,  $H\alpha$  center and the wings at  $\pm 0.5$ ,  $\pm 0.8$ , and  $\pm 1.2$  Å. The time cadence is 2 minutes for each wavelength during the impulsive phase of the flare, and the pixel size is 0.56". Such full-disk and multi-wavelength observation with high cadence is suitable to detect Moreton waves (e.g. Narukage et al. 2008). The Moreton wave was seen only from 08:02 UT to 08:08 UT with the SMART data. Figure 1 shows the Moreton wave in  $H\alpha$  center images taken by SMART. It mainly traveled in the south direction from the flare site. We derived the propagation speed by following the fastest wavefront. The mean propagation speed during the 6-minute appearance of the Moreton wave was about 760 km s<sup>-1</sup>. The  $H\alpha$   $-1.2$  Å images taken with SMART show the ejection of a filament with

the velocity of about  $300 \text{ km s}^{-1}$  in the direction of the Moreton wave<sup>1</sup>.

To compare the physical features of  $\text{H}\alpha$  Moreton waves with wave-like phenomena observed in EUVs, we used EUV images taken by *SDO/AIA*. In this letter we mainly used the  $193 \text{ \AA}$  images, which are mainly attributed to the  $\text{Fe XII}$  ( $\log(T) \sim 6.1$ ) line. The temporal resolution of the AIA  $193 \text{ \AA}$  data during the flare was 12 second. The flare site was close to the west limb. We also used EUV images taken by the Extreme-Ultraviolet Imager (EUVI) of the Sun Earth Connection Corona and Heliospheric Investigation (SECCHI; Howard et al. 2008) on board the *Solar Terrestrial Relations Observatory (STEREO; Kaiser et al. 2008)-Ahead* satellite (*STEREO-A*). The *STEREO-A* was  $\sim 100.7^\circ$  ahead of the earth at the time of the flare. The temporal resolutions of the  $195 \text{ \AA}$  and  $304 \text{ \AA}$  data, which we used in this letter, were 5 and 10 minutes, respectively. The pixel size of the images is  $1.58''$ .

Figure 2 shows the wave propagation seen in the *SDO/AIA*  $193 \text{ \AA}$  images (*top*) and in the *STEREO-A/EUVI*  $195 \text{ \AA}$  images (*bottom*). All are difference images, and are subtracted by the intensity maps taken at 07:55:19 and 07:55:31 UT for AIA and EUV data, respectively. The right panels of Figure 2 show the potential magnetic field lines for the view from the earth (*top*) and from the *STEREO-A* (*bottom*). The potential magnetic field lines are calculated by using synoptic magnetograms from GONG data<sup>2</sup> and based on the method by Shiota et al. (2008). In the images at 08:05 UT we can identify sharp wave fronts traveling southward, like as reported by Thompson et al. (2000), while the sharp fronts disappear after 08:10 UT. The EIT wave was blocked by small ARs in traveling, and did not show the isotropic feature. The magnetic field of the southern region of the flare site is weak. A part of the EUV wave traveling southward, which is shown with the arrows in Figure 2, traveled without being disturbed by such ARs. The propagation velocity of about  $700 \text{ km s}^{-1}$  was measured by following the wavefronts in the images. The wave front is much fainter than the sharp front seen at 08:05 UT.

### 3. Analysis and Results

In Figure 3(a) and (b) we showed the comparison of the spatial structure of the Moreton wave with that of the EUV wave of this flare. These are the difference images in AIA  $193 \text{ \AA}$  and in SMART  $\text{H}\alpha$  center, respectively. The time difference is noted in the Figure. The plus (+) signs follow the front of the Moreton wave. The front is well coincident with the sharp

---

<sup>1</sup>see, [http://www.kwasan.kyoto-u.ac.jp/topics/110809/bin\\_p12/](http://www.kwasan.kyoto-u.ac.jp/topics/110809/bin_p12/)

<sup>2</sup><http://gong.nso.edu/data/magmap/>

bright EUV wave front. In addition, we can identify an expanding dome on the wave front in AIA EUV images. Therefore, the expanding dome is thought to be the shock traveling in the corona, and the Moreton wave and the sharp EUV wave are the intersection with the chromosphere.

We examined the temporal features of the EUV wave, by using the time-distance diagrams (time-slice images) along the lines shown in the Figure 3(a). Figure 3(c), (d), and (e) are the time-slice images for the Line 1, 2, and 3, respectively. For each diagram, the flare site was set to be zero. The velocities were derived by following the features in the time-slice diagrams. The Line 1, which is drawn with a straight line mainly follows the dome structure expanding in the corona. In the time-slice images (Figure 3c) we can see a bright front (F1) with the traveling velocity of about  $760 \text{ km s}^{-1}$ , while it is initially even faster. Behind the front, we can identify the dimming feature. The Line 2 mainly follows the same path of the Moreton wave, and is following a great circle of the solar surface from the flare site. The front is very bright and sharp from 08:01 to 08:09 UT (F2b), which is almost the same time range of the Moreton wave. Even after 08:09 UT, we can identify the wave front, while it became much fainter (F2f). The traveling velocities are about  $730$  and  $620 \text{ km s}^{-1}$  for F2b and F2f, respectively. On the other hand, the bright edge is rapidly decelerated (S2b) and disappears at 08:12 UT. We also draw the Line 3 that also follows a great circle of the solar surface. Although the direction of the Line 3 is out of the arc of the Moreton wave front, we can see a wave-like feature. The propagation velocity of the bright front is initially about  $550 \text{ km s}^{-1}$  (F3b), and slow down to be about  $340 \text{ km s}^{-1}$  (S3b) after 08:06 UT. The slow bright EUV wave (S3b) suddenly disappears at about 08:12 UT. On the other hand, we can identify a fast faint feature (F3f) from 08:06 UT. The velocity is about  $580 \text{ km s}^{-1}$ . As we mentioned above, there are small ARs on the passes of the EUV waves. These small closed loops start to oscillate due to the propagation of the coronal wave. Along the Line 2 and 3, we can identify some oscillations as shown with the white arrows in Figure 3(d) and (e).

Associated with the flare, we observed the oscillations of a prominence on the west limb and a filament on the disk. The sites of the prominence/filament are shown in the left panel of Figure 1, with the characters P (prominence) and F (filament), respectively. In Figure 4 we show the temporal evolution of the limb prominence (P) in  $H\alpha$ s and in EUV ( $193 \text{ \AA}$ ) taken by SMART and AIA. From the SMART  $H\alpha$  wing data, we can clearly see the prominence moving in the line of the sight. First, the prominence became bright in the plus wing. The initial sign of the oscillation is identified with the darkening of the prominence in the  $-0.5 \text{ \AA}$  image taken at 08:11:57 UT. In the sequence of 08:14 UT, (at least, a part of) the prominence is the brightest in the most redward wing image of the observation, i.e.  $+1.2 \text{ \AA}$  image (08:14:24 UT). This means that the prominence is moving away with Doppler velocity of about  $50 \text{ km s}^{-1}$  or even faster. After this, the motion of the prominence

turned to be blueward, and in the sequence of 08:22 UT, it is brightest in the  $-1.2 \text{ \AA}$  images (08:21:45 UT). The oscillation period is roughly 15 minutes. In the AIA EUV images, on the other hand, we can also see the motion in the plane. First, it moves southward (downward in the images), then moves northward (upward) after 08:17 UT. The oscillation period is about 12 – 16 minutes, and the amplitude is about 10,000 km. The apparent velocity is about  $30 \text{ km s}^{-1}$ . In Figure 5(a) we show the time-slice image of the oscillating prominence in EUV ( $193 \text{ \AA}$ ) overlaid with the brightest points of the prominence in the  $\text{H}\alpha$  center images (the plot of the + sings). The slit position is shown in Figure 4. The prominence oscillation is identified as a filament oscillation in the *STEREO-A*/EUVI  $304 \text{ \AA}$  images, and we used the images to determine the precise distance from the flare site. From the start time of the oscillation and the site of the prominence, the coronal wave propagating with the velocity of about  $800 \text{ km s}^{-1}$  is expected to activate the prominence.

The filament on the disk F also showed oscillation features, although the features are much weaker both in the line-of-the-sight direction and in the plane than those for the prominence P. The start of the oscillation is roughly estimated as 08:17:57 UT from the  $\text{H}\alpha$  wing images. The oscillation period is about 15 minutes. We have to note that we can identify small activation at the footpoints of the filament F at 08:01:31 UT. Therefore, some weak movements of the filament already started when the coronal disturbance arrived at the filament. From the start time of the oscillation and the site of the filament, we expect the coronal wave propagating with the velocity of about  $570 \text{ km s}^{-1}$ .

#### 4. Summary and Conclusions

We simultaneously observed the  $\text{H}\alpha$  Moreton wave and the corresponding EUV fast coronal wave. The Moreton wave front was well consistent with the fast-bright-sharp EUV wave front (F2b). Even after the Moreton wave disappeared, we identified the propagation of the fast-faint EUV wave (F2f). Even along the Line 3 (Figure 3a), which is the direction without the Moreton wave, we found that the fast EUV waves (F3b, F3f). The fast EUV waves (F1, F2f, F3b, and F3f) are thought to be the fast-mode MHD waves (coronal waves). The EUV fast coronal waves appear more frequently than Moreton wave, although they are very faint and have not been observed until the launch of *SDO*. Especially, only when the shock strongly contacts with the chromosphere, the intersection is observed as the Moreton wave (F2b). The temporal evolutions of the  $\text{H}\alpha$  Moreton wave and the EUV waves are summarized in Figure 5(b).

In Figure 5 we also show the temporal evolutions of a type-II radio burst associated with the flare. In the metric radio spectrogram (25 – 2500 MHz) observed with the Hiraio Radio



Spectrograph (HiRAS; Kondo et al. 1995), we identify the type-II radio burst from 08:02:40 to 08:06:30 UT. Assuming the coronal density model proposed by Newkirk (1961) and Mann et al. (1999), we derived the propagation velocity of about  $850 \text{ km s}^{-1}$ . The observed type-II radio burst seems to be consistent with the Moreton wave and fast bright EUV wave, which also supports the interpretation of the wave as a fast-mode MHD shock.

We also found oscillations of a prominence and a filament. To trigger the oscillations by a flare-associated coronal disturbance, we expect a coronal wave as fast as the fast-mode MHD wave with the velocity of about  $570 - 800 \text{ km s}^{-1}$ . These velocities are consistent with the propagation velocities of the observed Moreton wave and the EUV fast coronal wave. An invisible Moreton wave could be such an EUV fast-faint coronal wave. It is known that a typical slow EIT wave sometimes causes filament oscillations (Okamoto et al. 2004), or such filament oscillations triggered by an EIT wave are expected to be stronger than those by an invisible Moreton wave (P. F. Chen, private communication). In the current case, however, the role of the EIT wave on the filament/prominence oscillations is unclear.

Along the Line 2 and 3, we identified slow-bright EUV waves (S2b, S3b) behind the fast-faint EUV waves. From the propagating features (i.e. the velocity and the isotropic propagation; Figure 2), we think it is a typical EIT wave. We simultaneously observed the EIT wave and the EUV fast wave (fast-mode MHD wave) as reported by Chen & Wu (2011). This means that the EIT wave is different from a fast-mode MHD wave, which supports the field-line stretching model (Chen et al. 2002, 2005). It is, however, difficult to clearly identify both features separately in the very initial phase of the flare, and it is unclear the relation between the fast-bright (F3f) and the slow-bright (S3b) EUV waves along the Line 3.

There is an alternative possibility that we observed a single coronal disturbance, and the two different waves (F2f/F3f and S2b/S3b) correspond to the fronts of two different heights (faster ones are higher) of the disturbance (Veronig et al. 2008; Warmuth & Mann 2011).

We, however, do not think the possibility due to the following reasons: First, the slow bright waves (S2b, S3b) stopped propagating at small active regions. This conflicts with the features of a fast-mode wave, while this is possibly reconciled by considering the stopping front as CME flanks as reported by Patsourakos & Vourlidas (2009). Second, we observed the prominence/filament oscillations. Since they are located low in the corona, we can derive the velocity of the shocks/waves there, from the distances and the times of the oscillations. In the current case we need waves with velocities of  $570 \text{ km s}^{-1}$  or more. Especially, the direction of the filament is close to the Line 3, and the required velocity is much faster than the bright slow wave (S3b), while it is consistent with the fast faint wave (F3f).

We thank the referee for the useful comments. This work is supported by KAKENHI



(23340045), and by the Global COE Program “The Next Generation of Physics, Spun from Universality and Emergence” from MEXT, Japan.

## REFERENCES

- Asai, A., Hara, H., Watanabe, T., Imada, S., Sakao, T., Narukage, N., Culhane, J. L., Doschek, G. A. 2008, *ApJ*, 685, 622
- Chen, P. F., Wu, S. T., Shibata, K., Fang, C. 2002, *ApJ*, 572, L99
- Chen, P. F., Fang, C., Shibata, K. 2005, *ApJ*, 622, 1202
- Chen, P. F., Wu, Y. 2011, *ApJ*, 732, L20
- Delannée & Aulanier 1999 *Sol. Phys.*, 190, 107
- Eto, S., et al. 2002, *PASJ*, 54, 481
- Gallagher, P. T. & Long, D. M. 2010, *Space Sci. Rev.*, 158, 365
- Harra, L. K., Sterling, A. C., Gömöry, P., Veronig, A. 2011, *ApJ*, 737, L4
- Hershaw, J., Foullon, C., Nakariakov, V. M., Verwichte, E. 2011, *A&A*, 531, id.A53
- Kai, K. 1970, *Sol. Phys.*, 11, 310
- Kaiser, M. L., Kucera, T. A., Davila, J. M., St. Cyr, O. C., Guhathakurta, M., Christian, E. 2008, *Space Sci. Rev.*, 163, 5
- Khan, J. I. & Aurass, H. 2002, *A&A*, 383, 1018
- Khan, J. I. & Hudson, H. S. 2000, *Geophys. Res. Lett.*, 27, 1083
- Klassen, A., Aurass, H., Mann, G., Thompson, B. J. 2000, *A&AS*, 141, 357
- Kondo, T., Isobe, T., Igi, S., Watari, S., Tokumaru, M. 1995, *J. Commun. Res. Lab.*, 42, 111
- Lemen, J. R., et al. 2011, *Sol. Phys.*
- Liu, W., Nitta, N. V., Schrijver, C. J., Title, A. M., Tarbell, T. D. 2010, *ApJ*, 723, L53
- Ma, S., Raymond, J. C., Golub, L., Lin, J., Ghen, H., Grigis, P., Testa, P., Long, D. 2011, *ApJ*, 738, 160

- Mann, G., Jansen, F., MacDowall, R. J., Kaiser, M. L., Stone, R. G. 1999 *A&A*, 348, 614
- Moreton, G. E. 1960, *AJ*, 65, 494
- Narukage, N., Hudson, H. S., Morimoto, T., Akiyama, S., Kitai, R., Kurokawa, H., Shibata, K. 2002, *ApJ*, 572, L109
- Narukage, N., Morimoto, T., Kadota, M., Kitai, R., Kurokawa, H., Shibata, K. 2004, *PASJ*, 56, L5
- Narukage, N., Ishii, T. T., Nagata, S., UeNo, S., Kitai, R., Kurokawa, H., Akioka, M., Shibata, K. 2008, *ApJ*, 684, L45
- Newkirk, G. Jr., *ApJ*, 133, 983
- Okamoto, T. J., Nakai, H., Keiyama, A., Narukage, N., UeNo, S., Kitai, R., Kurokawa, H., Shibata, K. 2004, *ApJ*, 608, 1124
- Patsourakos, S. & Vourlidas, A. 2009, *ApJ*, 700, L182
- Shibata, K., et al. 2011, *Solar Activity in 1992-2003*, (Kyoto: Kyoto University Press)
- Shiota, D., Kusano, K., Miyoshi, T., Nishikawa, N., Shibata, K. 2008, *J. Geophys. Res.*, 113, A03S05
- Smith, S. F. & Harvey, K. L. 1971, in *Physics of the Solar Corona*, ed. C. J. Macris (Dordrecht: Reidel), 156
- Thompson, B. J., et al. 1999, *ApJ*, 517, L151
- Thompson, B. J., Reynolds, B., Aurass, H., Gopalswamy, N., Gurman, J. B., Hudson, H. S., Martin, S. F., St. Cyr, O. C. 2000, *Sol. Phys.*, 193, 161
- Thompson, B. J. & Myers, D. C. 2009, *ApJS*, 183, 225
- Title, A., & AIA team 2006, *BAAS*, 38, 261
- Tripathi, D., Isobe, H., Jain, R. 2009, *Space Sci. Rev.*, 149, 283
- Uchida, Y. 1968, *Sol. Phys.*, 4, 30
- UeNo, S., Nagata, S., Kitai, R., Kurokawa, H., Ichimoto, K. 2004, *Proc. SPIE*, 5492, 958
- Veronig, A. M., Temmer, M., Vršnak, B. 2008, *ApJ*, 681, L113

Warmuth, A., Vršnak, B., Magdalenić, J., Hanslmeier, A., Otruba, W. 2004a, *A&A*, 418, 1101

—, —, —, —, — 2004b, *A&A*, 418, 1117

Warmuth, A. 2007, in *The High Energy Solar Corona: Waves, Eruptions, Particles* (Lecture Notes in Physics, Vol. 725), ed. K. L. Klein & A. L. Mackinnon (Berlin: Springer), 107

Warmuth, A. & Mann, G. 2011, *A&A*, 532, 151

Wills-Davey, M. J. & Attrill, G. D. R. 2009, *Space Sci. Rev.*, 149, 325

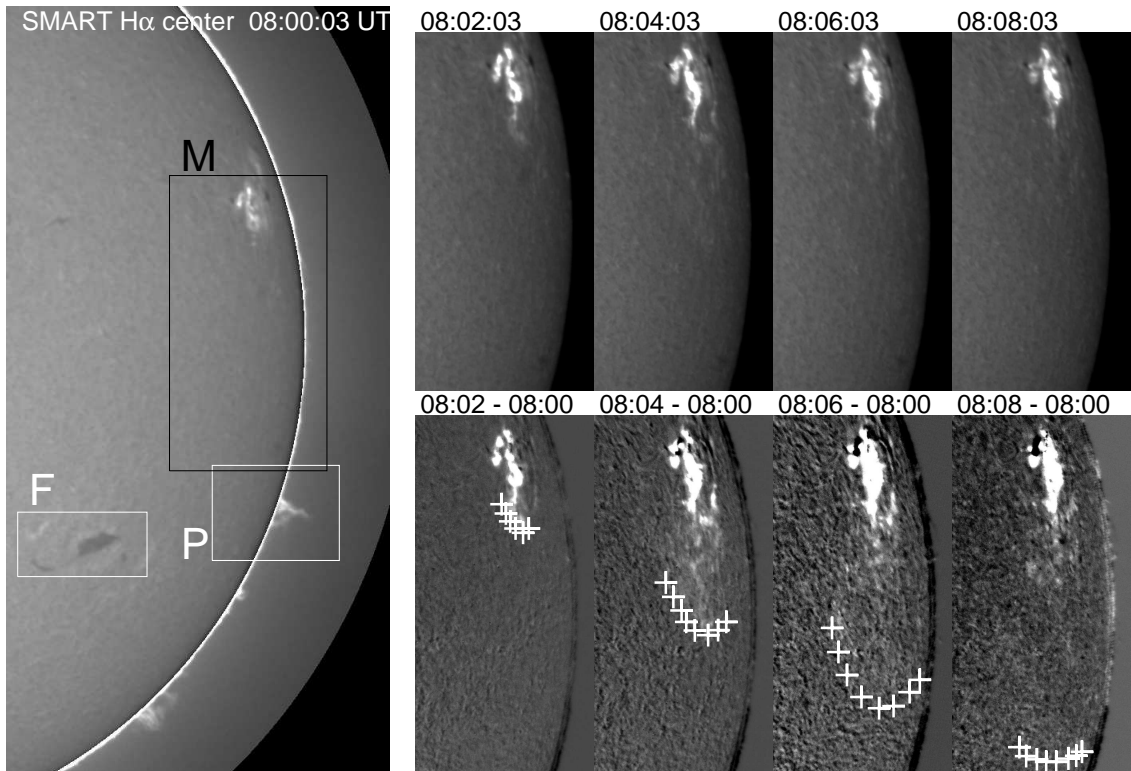


Fig. 1.— Propagation of the Moreton wave observed with SMART. Solar north is up and west to the right. The top right panels are the sequence of H $\alpha$  images of the region “M” (the black rectangle) in the left panel. The bottom right panels are the same sequence of the H $\alpha$  images but are subtracted with the image at 08:00 UT. The white rectangles with marks “P” and “F” in the left panel indicate the oscillated prominence and filament, respectively.



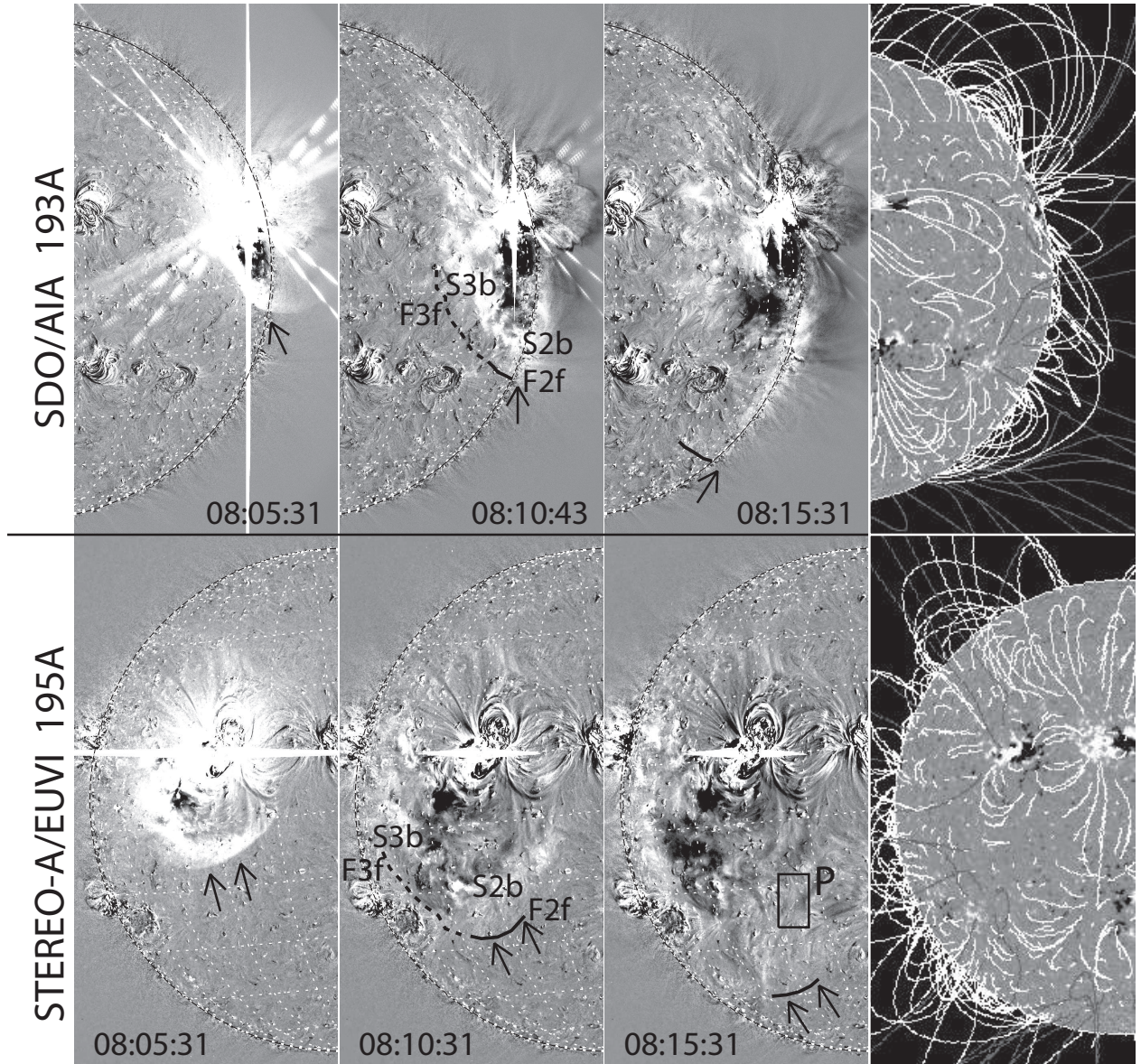


Fig. 2.— EUV waves observed with *SDO/AIA* 193 Å (*top*) and *STEREO-A/SECCHI/EUVI* 195 Å (*bottom*). The arrows follow the front of the EUV fast coronal wave. The region with mark P points the position of the limb prominence. The right panels show the potential magnetic field lines for the views from the earth (*top right*) and from the *STEREO-A* (*bottom right*).



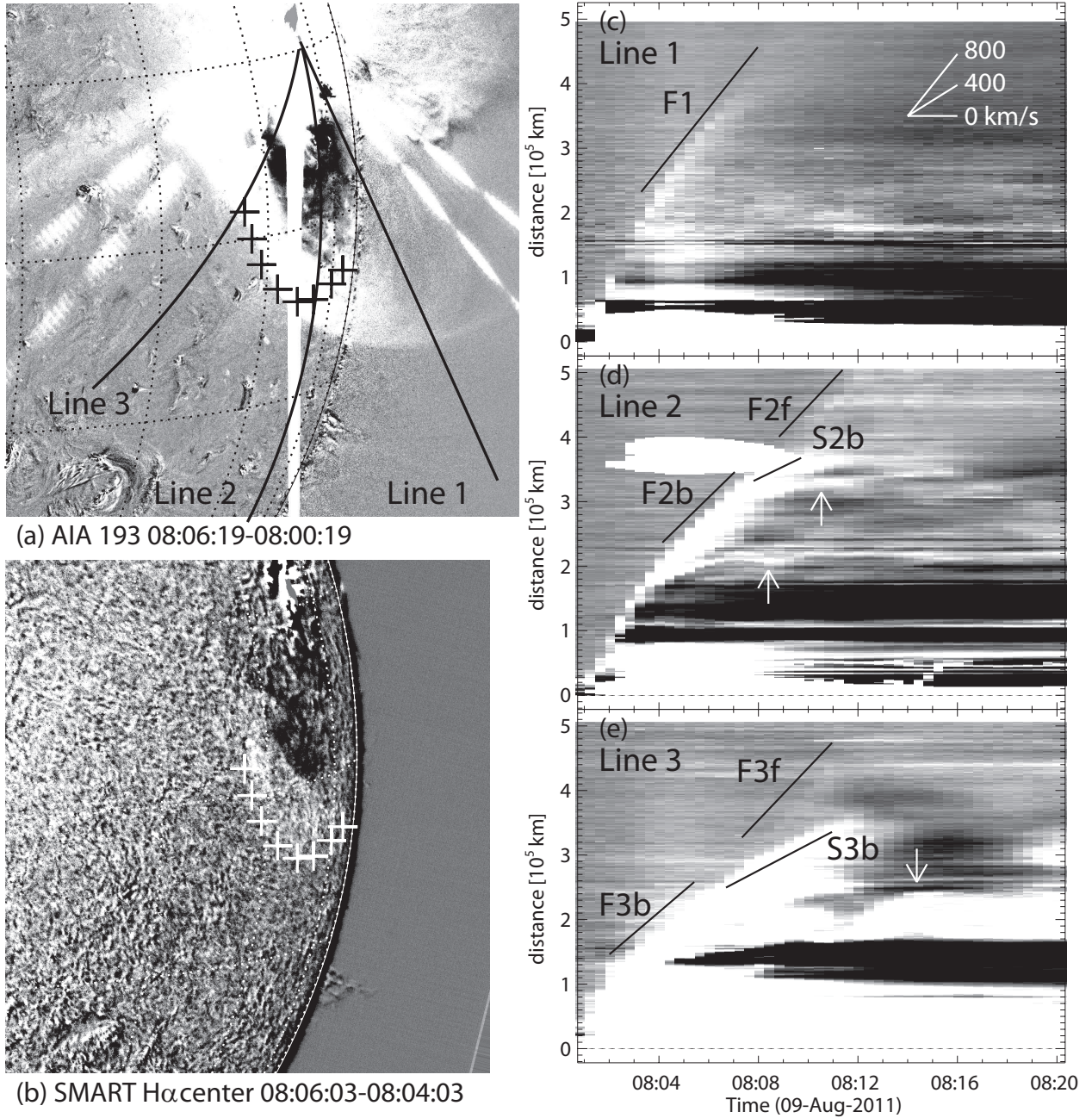


Fig. 3.— Detailed feature of coronal disturbances. (a) A difference image (08:06:19–08:00:19 UT) of EUV 193 Å image taken by *SDO/AIA*, and (b) a difference image (08:06:03–08:04:03 UT) of H $\alpha$  center image taken by SMART. The plus (+) signs follow the Moreton wave front. (c ~ e) Time-distance diagrams (time-slice images) of the AIA EUV 193 Å image along the line 1, 2, and 3, respectively. The lines are shown in (a). The solid lines marked with F1, F2b, F2f, F3b, F3f, and S3b follow EUV wave fronts: F (Fast) or S (Slow), the number of the line, and b (bright) or f (faint). The white arrows point the oscillating features caused during the propagation of the EUV waves.

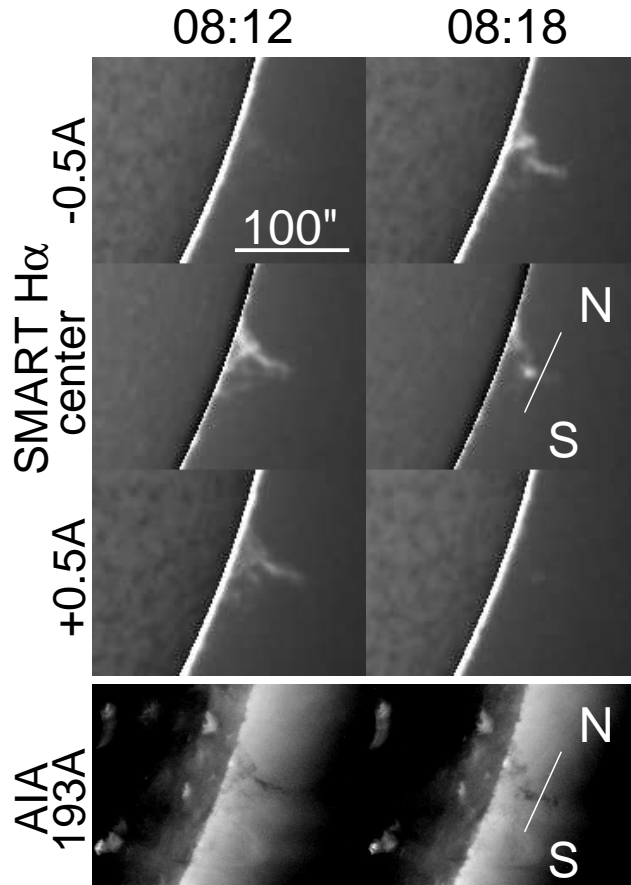


Fig. 4.— Temporal evolution of the oscillating prominence. *From top to bottom:*  $H\alpha$   $-0.5$  Å, center images, and  $+0.5$  Å images taken by SMART, and EUV  $193$  Å images taken by *SDO/AIA*. The field of view of each panels is the region P shown in Figure 1. The times (UT) are indicated on the top.



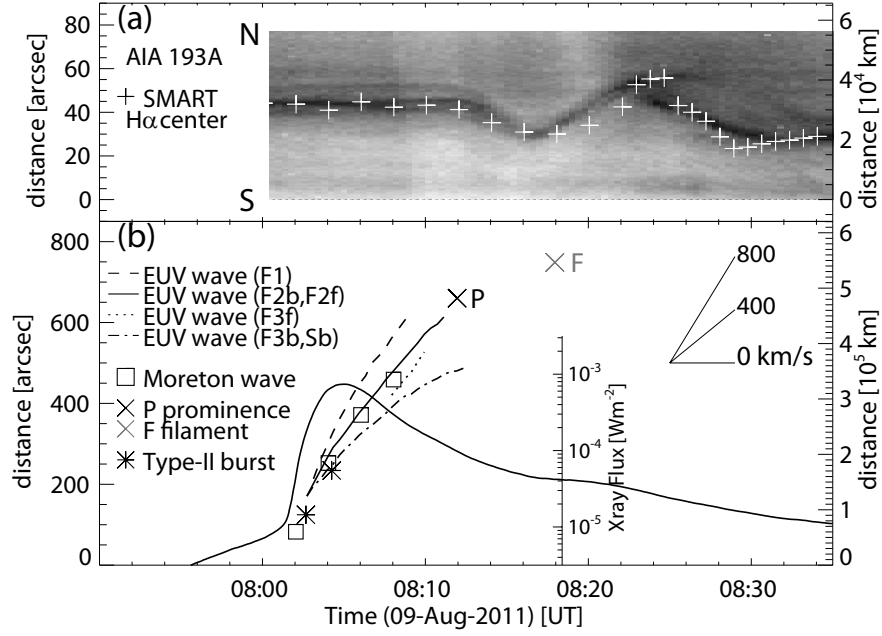


Fig. 5.— Height-time evolution of the flare-related phenomena. (a) A time-distance diagram (time-slice image) of the AIA EUV 193 Å image along the slit line shown in the Figure 4. N and S show the north and south directions, respectively. The brightest points of the prominence in the H $\alpha$  center images are overlaid with the plus (+) signs. (b) Temporal evolutions of the EUV waves, the Moreton wave, and the type-II radio burst with GOES X-ray flux at the 1 – 8 Å channel. The distance of the Moreton wave front ( $\square$ ) was measured along a great circle of the solar surface from the flare site. The EUV wave fronts measured with the Line 1, 2, and 3 (see, Figure 3) are shown with the dashed, solid, and dash-dot lines, respectively. The fast faint EUV wave seen in the Line 3 (F3f) is also shown with the dotted line. The times and distances of the oscillating limb prominence (P) and disk filament (F) are shown with the cross ( $\times$ ) signs. The distance of the type-II radio burst (\*) was calculated, by using a coronal electron density model, and the zero was set to be the photosphere.